# Development of a robot-aided modal analysis measurement method using laser Doppler vibrometry

**O. Devigne** [1], **S. Hoffait** [2], **O. Brüls** [1]
[1] University of Liège, Department of Aerospace & Mechanical Engineering,
Allée de la Découverte 9, B-4000, Liège, Belgium
e-mail: **o.devigne@uliege.be**

[2] V2i SA, Research & Development Department,
Avenue du Pré-Aily 25, B-4000, Liège, Belgium

## Abstract
In this paper, a robot-assisted modal analysis method is developed. A laser Doppler vibrometer (LDV) is mounted on an industrial robot with the objectives of gaining time and accuracy in the point-to-point movement of the LDV and getting the ability to perform precise contactless 3D measurements.
Firstly, a calibration procedure is needed to define the positions and orientations of the laser beam and the studied mechanical structure with respect to the robot frame. The proposed solution consists in adapting a common tool calibration method based on physical contact by the introduction of an intermediate device.
Secondly, modal analyses using both mono- (1D) and multi-directional (3D) measurements are performed on an academic compressor wheel. The 1D analysis demonstrates the accuracy and the time gain that the robot offers compared to a manual operation, whereas the 3D analysis highlights a significant reduction in spatial aliasing in comparison to 1D measurements.

## 1 Introduction

In the field of vibration testing, modal analysis methods can rely on sensors directly attached to the structure to be tested, such as accelerometers, or on contactless sensors.

In the first case, an excitation is applied to the structure at one or several points and the response is recorded using one or several sensors. In the case of an impact hammer excitation, the impulse can be applied at different locations while keeping the sensor fixed. This technique is called the "roving hammer". The other possibility is to work with the "roving sensor", where the excitation keeps a fixed location and the sensor is moved on the structure. In the case of ground vibration testing (*e.g.* with a shaker excitation), the roving sensor is used. These techniques allow one to compute lines or columns of the FRF matrix

$$\mathbf{H}(\omega) = \begin{bmatrix} H_{11} & H_{12} & \cdots & H_{1s} \\ H_{21} & H_{22} & \cdots & H_{2s} \\ \vdots & \vdots & \ddots & \vdots \\ H_{r1} & H_{r2} & \cdots & H_{rs} \end{bmatrix}. \tag{1}$$

In this matrix, each element $H_{rs}$ is the FRF containing the response of the structure at degree of freedom $r$ due to an excitation at degree of freedom $s$. When using only one sensor, this process is time consuming, since the impact or the sensor has to be moved a high number of times. When using several sensors, the additional mass becomes problematic for light structures, since it can significantly change their dynamic behavior.

In the second case, contactless sensors such as laser Doppler vibrometers (LDV) are used. The dynamics of the structure is thus preserved and the same "roving sensor" method can be used. A common type of LDV

is the single-beam arrangement which measures the velocities along the line of sight by using the Doppler shift of the reflected beam. This is the LDV which is used in this work. An infrared laser beam is sometimes used in order to avoid using special reflective tape on the studied part.

If there is only one sensor, this sensor (or the mechanical structure itself) must be precisely moved to multiply the measurements. A solution is to make use of a moving set of mirrors [1, 2] allowing the in-plane movement of the laser beam. This arrangement is called a scanning laser Doppler vibrometer (SLDV). However, the analysis of more complex parts, such as compressor blades is still challenging, because keeping the same beam orientation for every measurement point is not sufficient due to the complexity of the encountered mode shapes. Moreover, this equipment is more expensive than an LDV.

Performing a human-operated modal analysis on a complete compressor wheel using an LDV is thus a tedious operation. Indeed, the LDV must be positioned with an accuracy in the order of the millimeter for each measurement point. A complete measurement campaign might take up to one week for this type of application. Moreover, performing 3D measurements becomes almost impossible because the angle between the LDV and the wheel cannot be precisely controlled.

The solution presented in this paper is to mount the vibrometer on an industrial robot so that the desired points can be easily reached. Furthermore, one gets the ability to perform precise 3D measurements. Of course, the path of the robot must be pre-programmed and the whole system must be well calibrated. This last aspect is extremely important. Indeed, the reference frame of the studied mechanical structure should be localized with respect to the reference frame of the robot. Moreover, the tool center point, representing the laser beam, should be localized with respect to the robot flange. This calibration is crucial in order to reach the correct position on the structure. The solution introduced in [3, 4] is interesting but the calibration technique adopted still relies on human subjectivity and is rather complex. In this paper, a simpler concept is proposed and evaluated.

Two objectives are followed. The first one is to prove the feasibility of performing accurate 1D and 3D measurements with an industrial robot. The second one is to check the overall time savings of the robotized solution.

The paper is organized as follows. Section 2 gives some background on the setup of the different reference frames needed to define the measurement points and the robot path. Section 3 focuses on the calibration of both the LDV and the mechanical structure with respect to the robot. Section 4 introduces the academic compressor wheel on which measurements are performed and its finite element (FE) model. In Section 5, the setup and results of 1D measurements on the structure are presented, as well as a discussion on the time gain offered by the robot. Section 6 highlights the advantages of performing 3D measurements. Conclusions and perspectives are given in Section 7.

# 2 Background

Before entering the details of the calibration procedure, some key concepts should be introduced. This section proposes a global view of the reference frames needed to define the measurement points and to perform the robot trajectory planning. It also presents useful robotics concepts, namely the tool center point, robot flange and world frame.

## 2.1 Definition of the measurement points

In the context of modal analysis, measurement points are often specified in the CAD file of the structure, and all data are given in this reference frame. The definition procedure is detailed here below.

1. The measurement points are chosen on the surface of the structure in the CAD environment.
2. Positions and orientations of the LDV are determined for each measurement point. To this end, a frame is introduced in the CAD environment, with its origin at the location of the measurement point. For

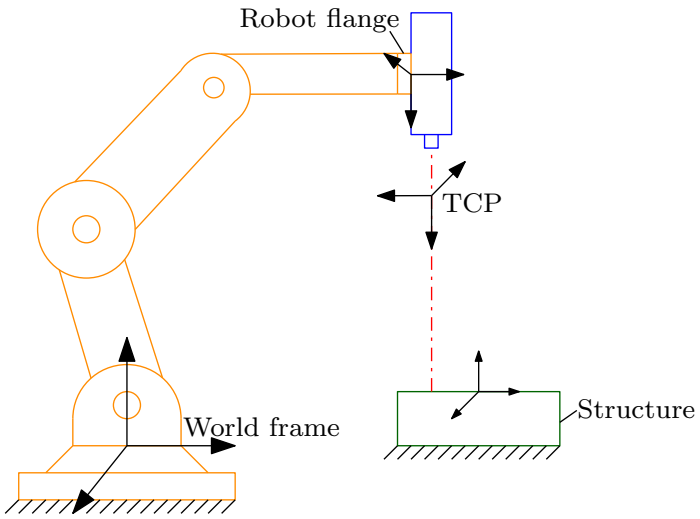


Figure 1: Robot-aided measurement system.

a 1D analysis, only the $z$-axis specifies the measurement direction. However, for a 3D analysis, each axis represents a measurement direction.

3. Through the knowledge of these measurement frames, positions and orientations can be extracted and expressed in the reference frame of the mechanical structure.

A first role of the calibration procedure is to introduce the position and orientation of the structure frame with respect to the robot frame, called "world frame", in order to be able to use the previously defined positions and orientations.

### 2.2 Definition of the tool

As illustrated in Figure 1, the LDV is fixed on the robot flange using an interface part. This interface is attached with 4 screws and two pins. In order to introduce the relative position and orientation of the LDV with respect to the robot flange, the tool center point (TCP) must be specified. The TCP of the robot is defined as a particular point along the laser beam and the $z$-axis of the TCP frame represents the direction of the beam.

The relative position and orientation of the TCP frame with respect to the robot flange should be determined precisely by calibration in order to program the trajectory of the robot so that the LDV reaches the planned measurement points.

## 3 Calibration

As previously mentioned, it is critical to know precisely the positions and orientations of both the TCP and the mechanical structure under study with respect to the robot. These two problems are complementary. In the first problem, the question is to specify the position and orientation of the TCP with respect to the frame of the robot flange. A common tool calibration method, which relies on a physical contact between the tool and a reference point in the workspace, is first reviewed. However, this approach cannot be used as such in our context, because the laser beam is not a material object. Therefore, an adaptation is proposed. In the second problem, the question is to specify the position and orientation of the mechanical structure with respect to the world frame of the robot.

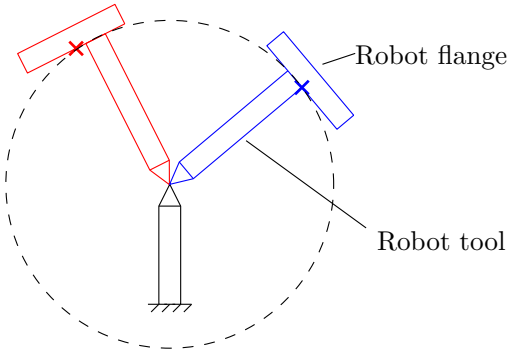


Figure 2: The flange center lies on a sphere when the tool is brought in contact with the reference point in different orientations (blue and red).

### 3.1 Physical TCP calibration

A common tool calibration method from the robotics field is first presented. It relies on physical contact of the tool to a reference point in the workspace (very often, a tip). In the following, a superscript will represent the reference frame in which the different quantities are expressed, while a subscript will describe the quantity itself: "f" for the flange, "w" for the world, and "CAD" for the structure. In order to define the TCP, the relative position ${}^{\mathrm{f}}\mathbf{x}_{\mathrm{TCP}}$ and orientation ${}^{\mathrm{f}}\mathbf{R}_{\mathrm{TCP}}$ with respect to the robot flange should be given. For the moment, let the reader focus on the determination of ${}^{\mathrm{f}}\mathbf{x}_{\mathrm{TCP}}$. The method is based on a reference point whose position ${}^{\mathrm{w}}\mathbf{x}_{\mathrm{c}}$ in the world frame is fixed but unknown. The tip of the tool is brought in contact with this reference point with different orientations such that ${}^{\mathrm{w}}\mathbf{x}_{\mathrm{TCP}} = {}^{\mathrm{w}}\mathbf{x}_{\mathrm{c}}$. The flange position ${}^{\mathrm{w}}\mathbf{x}_{\mathrm{f}}$ will be localized on a sphere centered at the reference point (*i.e.* the tip of the tool), as illustrated in Figure 2. The coordinates of the flange center in the world frame ${}^{\mathrm{w}}\mathbf{x}_{\mathrm{f}}$, as well as the rotation matrix ${}^{\mathrm{w}}\mathbf{R}_{\mathrm{f}}$ from the flange frame to the world frame are given by the robot. A set of $N$ measured points can thus be obtained so that one gets $N$ equations of the form

$$||{}^{\mathrm{w}}\mathbf{x}_{\mathrm{f}} - {}^{\mathrm{w}}\mathbf{x}_{\mathrm{c}}||^2 = R^2 \tag{2}$$

with $R$ the radius of the sphere.

By equation subtraction, this system of $N$ nonlinear equations can be transformed into a system of $N-1$ linear equations in ${}^{\mathrm{w}}\mathbf{x}_{\mathrm{c}}$. By solving the system with a linear least-squares method, the coordinates of the TCP ${}^{\mathrm{w}}\mathbf{x}_{\mathrm{TCP}} = {}^{\mathrm{w}}\mathbf{x}_{\mathrm{c}}$ can be found in the world frame. The position of the TCP with respect to the flange frame can then be obtained with the relation

$${}^{\mathrm{f}}\mathbf{x}_{\mathrm{TCP}} = {}^{\mathrm{f}}\mathbf{R}_{\mathrm{w}} \left({}^{\mathrm{w}}\mathbf{x}_{\mathrm{TCP}} - {}^{\mathrm{w}}\mathbf{x}_{\mathrm{f}}\right). \tag{3}$$

### 3.2 Non-physical TCP frame calibration

In our case, the TCP is defined on the laser beam of the LDV. The above method is not directly applicable because the laser beam is not a material object. It is thus not possible to bring it in contact with a reference point in the workspace. In [3, 4], a CMOS sensor is used. The idea is to jog the robot and orient the beam to the sensor, so that the laser spot can be seen on a computer screen. A fixed standoff distance of the LDV is used, so that the distance from the lens to the sensor is manually adjusted in order to get the smallest spot size on the screen. This method has two major drawbacks. The first one is that a CMOS sensor interfaced to work with a computer is needed. The second is that the method highly depends on the user's subjectivity, so that the final accuracy may be user-dependent.

The solution proposed here is simpler to set up and requires less subjective inputs from the user. It consists in introducing a removable intermediate tool, for instance, a tip. This tool is positioned on the LDV in such a way that the laser beam appears precisely on its extremity, as illustrated in Figure 3. Consequently, calibrating the LDV frame boils down to calibrating a physical tool as presented in the previous section.

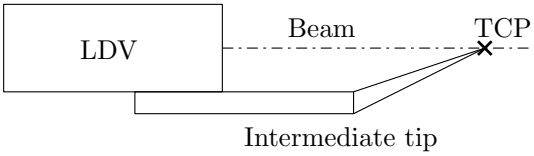


Figure 3: The intermediate tip extremity is positioned on the laser beam.

In order to obtain the rotation ${}^{\mathrm{f}}\mathbf{R}_{\mathrm{TCP}}$, the following procedure is then proposed. Knowing the sphere center ${}^{\mathrm{w}}\mathbf{x}_{\mathrm{c}}$ in the world frame from the calibration, one can generate points on a sphere of larger radius. The robot flange is then moved to these points and the beam is manually oriented to the reference point while keeping the flange center on the sphere surface. Using the above method, the TCP is then located at a new position ${}^{\mathrm{w}}\mathbf{x}^{\star}_{\mathrm{TCP}} \neq {}^{\mathrm{w}}\mathbf{x}_{\mathrm{c}}$. By the knowledge of the two points ${}^{\mathrm{f}}\mathbf{x}_{\mathrm{TCP}}$ and ${}^{\mathrm{f}}\mathbf{x}^{\star}_{\mathrm{TCP}}$, one can define the beam axis ${}^{\mathrm{f}}\mathbf{e}_{z,\,\mathrm{TCP}}$. Two other vectors ${}^{\mathrm{f}}\mathbf{e}_{x,\,\mathrm{TCP}}$ and ${}^{\mathrm{f}}\mathbf{e}_{y,\,\mathrm{TCP}}$ are then selected arbitrarily to form an orthonormal basis, from which the rotation matrix ${}^{\mathrm{f}}\mathbf{R}_{\mathrm{TCP}}$ is deduced, insuring the complete definition of the LDV frame by its position and orientation.

### 3.3 Mechanical structure frame calibration

With the above arrangement, the position ${}^{\mathrm{w}}\mathbf{x}_{\mathrm{CAD}}$ and orientation ${}^{\mathrm{w}}\mathbf{R}_{\mathrm{CAD}}$ of the structure frame with respect to the robot basis can be obtained by touching the structure at predefined points $i$ with the intermediate tip. Those points are chosen in the CAD environment and consist in easily reachable points (*e.g.* intersection of edges). By physical contact, their coordinates in the world frame ${}^{\mathrm{w}}\mathbf{x}_i$ are obtained. One can write for each point $i$

$$ {}^{\mathrm{w}}\mathbf{x}_i = {}^{\mathrm{w}}\mathbf{x}_{\mathrm{CAD}} + {}^{\mathrm{w}}\mathbf{R}_{\mathrm{CAD}}\,{}^{\mathrm{CAD}}\mathbf{x}_i. \tag{4} $$

It is possible to numerically evaluate ${}^{\mathrm{w}}\mathbf{x}_{\mathrm{CAD}}$ and ${}^{\mathrm{w}}\mathbf{R}_{\mathrm{CAD}}$ using a least-squares method [5]. The first step is to compute the centroids for each data set as follows

$$ {}^{\mathrm{w}}\mathbf{x}_o = \frac{1}{N}\sum_{i=1}^{N} {}^{\mathrm{w}}\mathbf{x}_i \tag{5} $$

and

$$ {}^{\mathrm{CAD}}\mathbf{x}_o = \frac{1}{N}\sum_{i=1}^{N} {}^{\mathrm{CAD}}\mathbf{x}_i. \tag{6} $$

In order to find a rotation matrix between the CAD and the world coordinates, the idea is to use the centroids to recenter both data sets. One can build a matrix $\mathbf{H}$, on which a singular value decomposition is performed, defined as

$$ \mathbf{H} = \sum_{i=1}^{N} \left({}^{\mathrm{CAD}}\mathbf{x}_i - {}^{\mathrm{CAD}}\mathbf{x}_o\right)\left({}^{\mathrm{w}}\mathbf{x}_i - {}^{\mathrm{w}}\mathbf{x}_o\right)^T = \mathbf{U}\mathbf{S}\mathbf{V}^T. \tag{7} $$

The rotation matrix is then obtained as

$$ {}^{\mathrm{w}}\mathbf{R}_{\mathrm{CAD}} = \mathbf{V}\mathbf{U}^T. \tag{8} $$

From this knowledge, the frame position is computed as

$$ {}^{\mathrm{w}}\mathbf{x}_{\mathrm{CAD}} = -{}^{\mathrm{w}}\mathbf{R}_{\mathrm{CAD}}\,{}^{\mathrm{CAD}}\mathbf{x}_o + {}^{\mathrm{w}}\mathbf{x}_o. \tag{9} $$

In terms of repeatability, the whole procedure exhibits an accuracy in the order of the millimeter after four calibrations of the LDV and the structure frames.

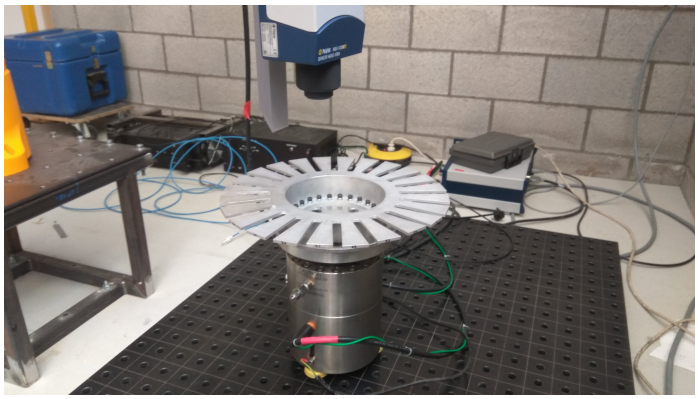

Figure 4: Measurement setup of the analyzed academic compressor wheel.

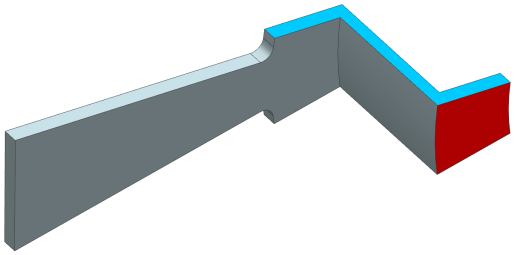

Figure 5: Boundary conditions of the sector. The red (bottom) face is fixed and the tangential degrees of freedom of the blue (side) face are blocked.

# 4 Test structure and FE model

The measurements are carried out on an academic compressor wheel, already used in [6], illustrated in Figure 4. An FE model of one sector of the structure is used for the comparison between the theoretical and experimental results. A modal analysis is performed with the boundary conditions depicted in Figure 5. The tangential degrees of freedom of the blue (side) face are blocked to represent the symmetry condition, and the red (bottom) face is fixed to represent the fixation to the shaker.

# 5 1D measurements

## 5.1 Setup

The structure is mounted on a piezoelectric shaker, so that a high-frequency analysis is possible. For the measurement phase, 10 burst random excitations are applied to the structure. The responses are then averaged. The analysis is performed using the software Siemens LMS Test.Lab. One blade is discretized in 33 points, as illustrated in Figure 6 and the measurement direction of the LDV is normal to the wheel surface at all time (according to the shown frames, in the $z$-direction). This setup emulates a typical vibration measurement procedure and allows one to compare the proposed robotized solution to a manual method.

## 5.2 Results

In Figure 7, one finds the MAC matrix between the reduced FE model and the experimental results up to 7460 Hz. It is clearly observed that some modes exhibit cross-correlation with each other. Noticeably, the experimental modes corresponding to the theoretical mode 2 correlate with the theoretical mode 3, the experimental modes corresponding to the theoretical mode 4 correlate with the theoretical modes 2 and 4,

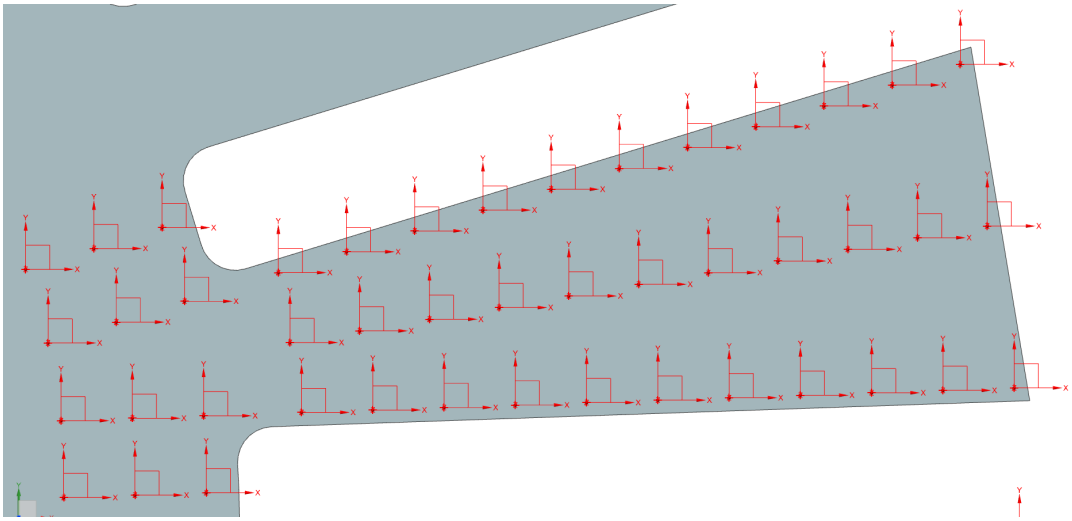

Figure 6: Measurement points locations for the 1D analysis.

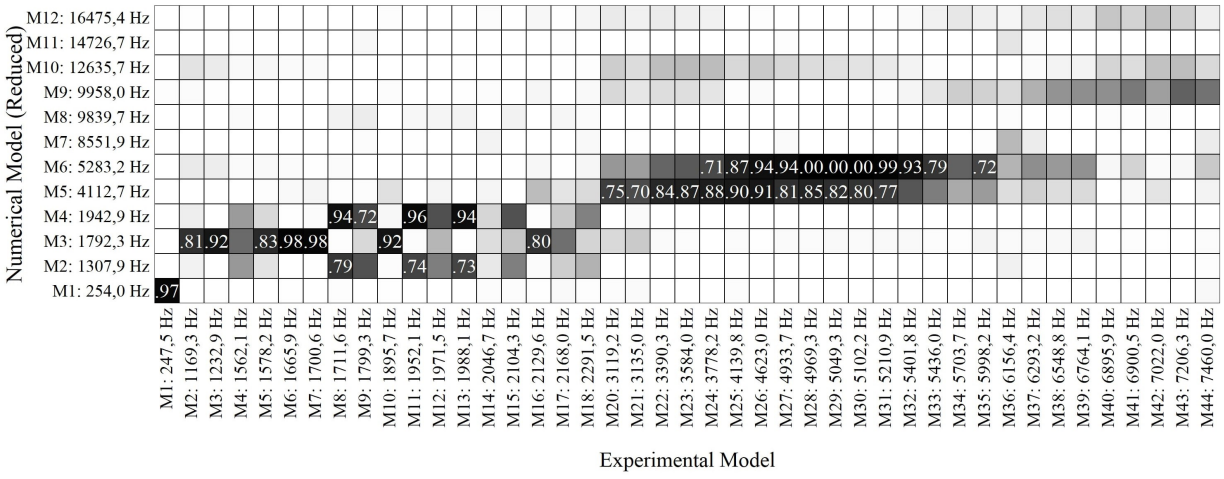


Figure 7: Results up to 7460 Hz (1D analysis).

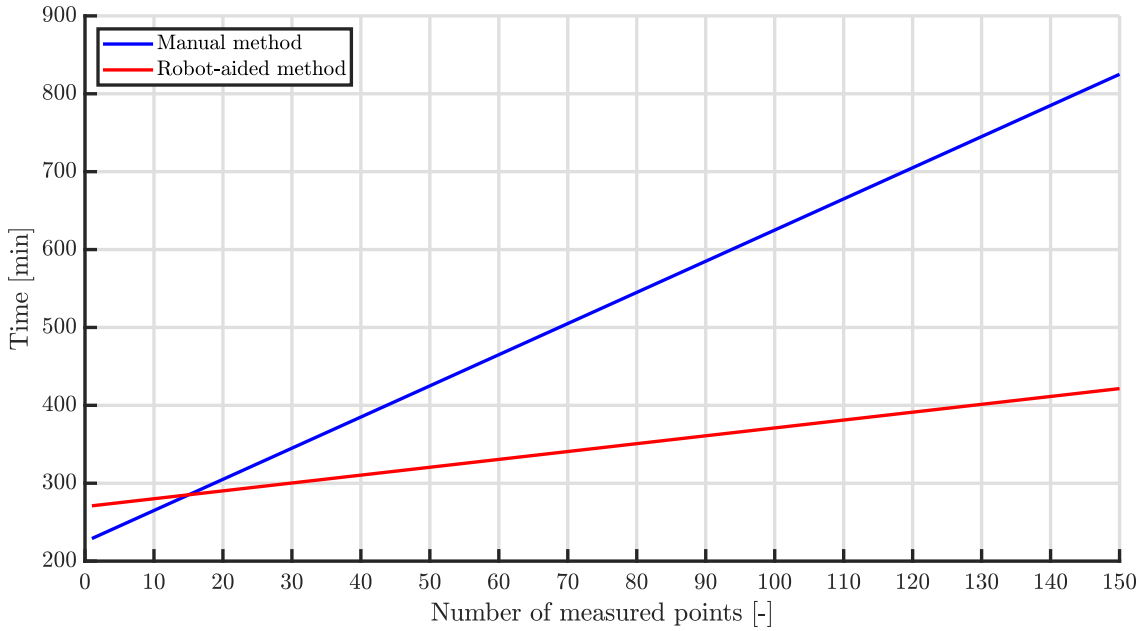


Figure 8: Total time as a function of the number of points for both the manual and the robot-aided methods.

Table 1: Estimation of the time taken for each operation of the modal analysis with and without the robot.

| | **Manual operation (min)** | **Robot operation (min)** |
|---|---|---|
| Setup (part + LDV) | 180 | 120 |
| Calibration (part + LDV) | - | 90 |
| Programming of the points | - | 60 |
| Measuring of the points | 45 | - |
| Measurement time | 1 | 1 |
| Point-to-point movement in 1D | 3 | 0.01 |
| **Total** | **229** | **271.01** |

and the experimental modes corresponding to the theoretical modes 5 and 6 are hardly differentiable. The reason of this behavior is explained in the next section, in light of the comparison with 3D measurements.

## 5.3 Discussion

One of the sought objectives of the robot-aided measurement procedure is to gain time with respect to a manual operation of the LDV. An estimation of the time cost of the individual steps of both procedures is shown in Table 1.

- The first step is the installation of the mechanical part and the LDV. Without the use of tripods or specific supports, this operation is less tedious with the robot.
- The next steps are the calibration and preprogramming of the measurement points. Obviously, without the use of the robot, these steps do not exist.
- Afterwards, for a manual operation, an approximate measurement position is chosen and then precisely measured, for instance, with the use of a measuring arm.
- The following step is the measurement itself, which requires a fixed time regardless of the used method.
- Finally, the LDV is moved to the next measurement location. This is the critical step. Indeed, the robot moves quite rapidly to a preprogrammed point, whereas a completely manual operation requires the user to precisely move the LDV and its support to its next position. This is why, although the use of the

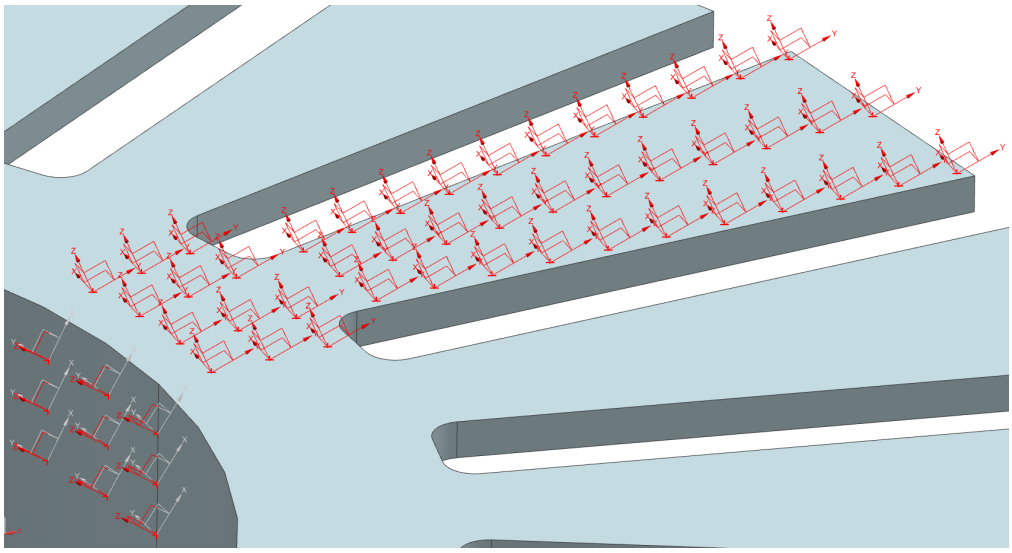

Figure 9: Measurement points locations and directions for the 3D analysis.

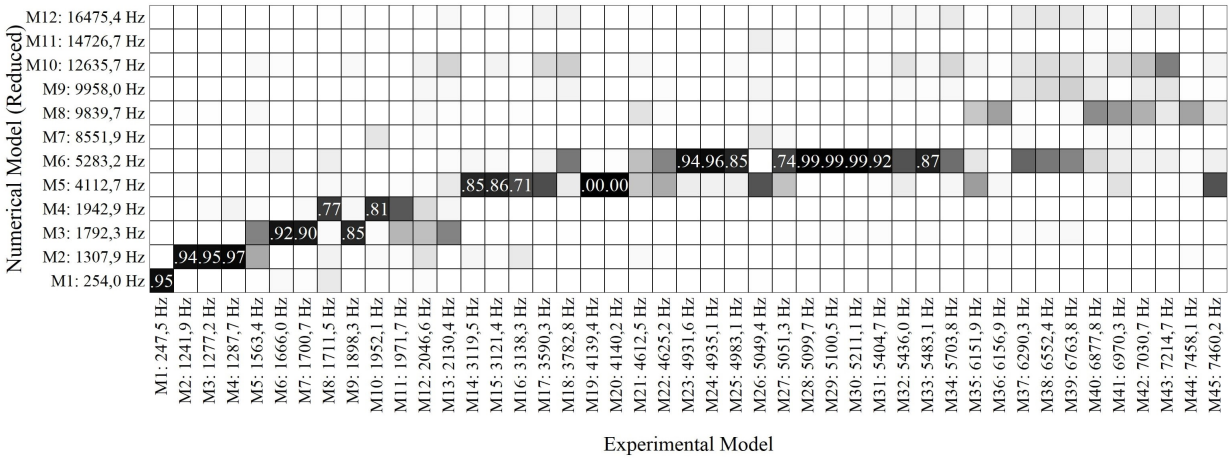


Figure 10: Results up to 7460 Hz (3D analysis).

robot is penalizing for a low number of measurement points, Figure 8 shows that it is actually beneficial for applications involving more than 15 points. The benefit would become particularly significant for large industrial applications, which often involve hundredths of measurement points.

# 6 3D measurements

## 6.1 Setup

The same setup as for the 1D measurements is used, *i.e.* the academic compressor wheel mounted on a piezoelectric shaker. However, the blade is now discretized using 45 points and the three measurement directions follow the axes of each frame depicted in Figure 9. Additionally, 12 monodirectional measurements are performed on the wheel drum, in the $z$-direction. A total number of 144 measurements are thus performed. This setup is practically impossible to achieve with a manual operation due to the lack of control of the laser beam orientation.

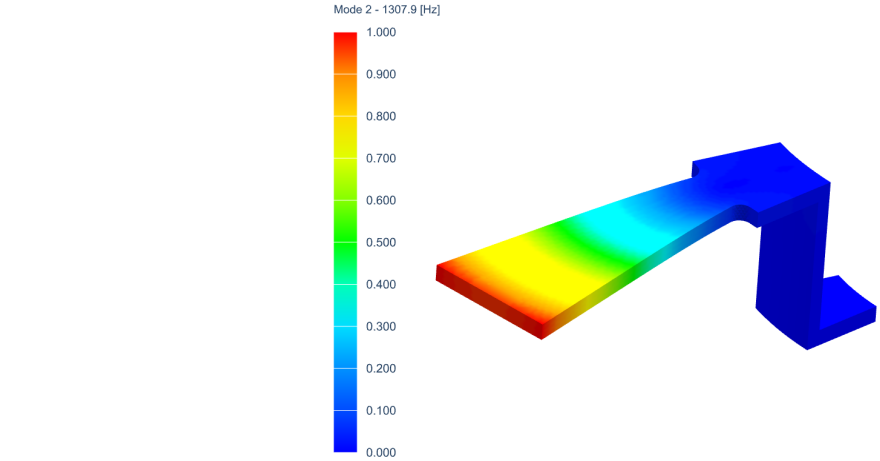


(a) Theoretical FE mode.

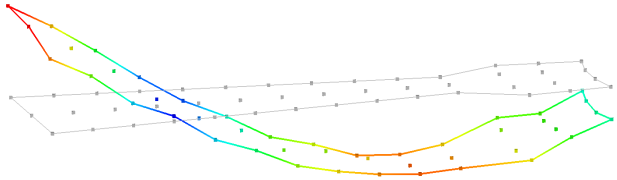

(b) Experimental mode (1D analysis).

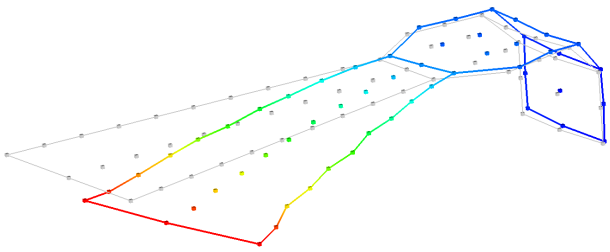

(c) Experimental mode (3D analysis).

Figure 11: Second mode shape of the structure.

### 6.2 Results and discussion

In Figure 10, one finds the MAC matrix between the reduced FE model and the experimental results up to 7460 Hz. As it can be seen, the spatial aliasing which was present in the 1D analysis for the theoretical modes 2 and 3 or the theoretical modes 5 and 6, among others, completely disappears with the introduction of two other measurement directions. This reveals the ability of the 3D analysis to capture an in-plane mode, and to precisely measure oriented points on the drum. Indeed, for the 1D analysis, the modal amplitudes are only available in the normal direction to the blade, so that the projections of the experimental modes corresponding to the theoretical mode 2, which is an in-plane mode, correlate with the first bending mode (theoretical mode 3). Thanks to the 3D analysis, this in-plane mode is completely recovered experimentally, as it can be observed in Figure 11. On the other hand, for the 1D analysis, the experimental modes corresponding to the theoretical mode 5 are correlated with the third bending mode (corresponding to the theoretical mode 6). The 3D analysis is able to experimentally reveal that the theoretical mode 5 is actually induced by the drum deformation. This is illustrated in Figure 12.

## 7 Conclusions and future work

This paper investigates the use of an industrial robot for contactless modal analysis using an LDV. A novel calibration method for the positioning of the LDV and the mechanical structure with respect to the robot was introduced. It only requires a calibration tip and an intermediate tip attached to the LDV.

This association of the robotics and vibration testing technologies presents several advantages. For a simple 1D analysis on an academic structure, the use of the robot induces a considerable time gain with respect to a manual operation. Moreover, multidirectional measurements can be performed, bringing to the fore a significant reduction in spatial aliasing compared to the 1D analysis. Indeed, it was noticeably possible to capture an in-plane mode by performing precisely oriented measurements.

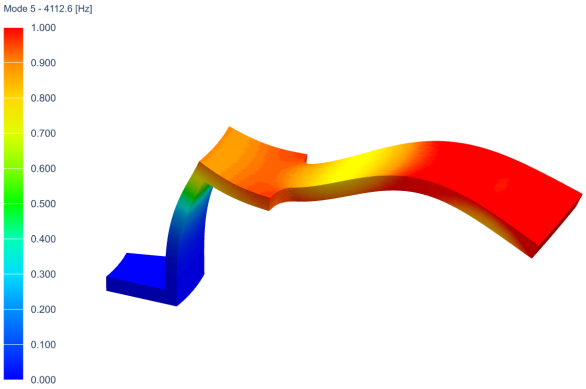


(a) Theoretical FE mode.

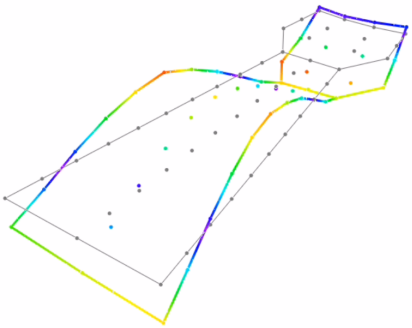

(b) Experimental mode (1D analysis).

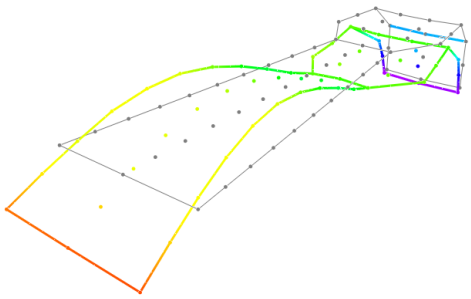

(c) Experimental mode (3D analysis).

Figure 12: Fifth mode shape of the structure.

As a perspective, an automation of the measurement process as well as an improvement of the calibration method is currently developed. This allows one to discretize the structure even more precisely, without the need of an operator to launch each measurement, while gaining even more time during the calibration phase. Consequently, overnight automated work would provide a considerable human and financial cost reduction, alongside with the improvement of the measurement quality.

## Acknowledgments

This work was partly supported by the Interreg Robotix Academy project of the Greater Region.

## References

[1] B. Stoffregen and A. Felske, "Scanning laser doppler vibration analysis system," *SAE Transactions*, pp. 934–940, 1985.

[2] M. Batel, "Deploying successfully laser doppler vibrometry techniques within the automotive nvh process," *Journal of the Acoustical Society of America*, vol. 123, no. 5, p. 3868, 2008.

[3] L. Bertini, P. Neri, C. Santus, and A. Guglielmo, "Automated experimental modal analysis of bladed wheels with an anthropomorphic robotic station," *Experimental Mechanics*, vol. 57, no. 2, pp. 273–285, 2017.

[4] L. Bertini, B. Monelli, P. Neri, C. Santus, and A. Guglielmo, "Robot assisted modal analysis on a stationary bladed wheel," in *ASME 2014 12th Biennial Conference on Engineering Systems Design and Analysis*. American Society of Mechanical Engineers Digital Collection, 2014.

[5] K. S. Arun, T. S. Huang, and S. D. Blostein, "Least-squares fitting of two 3-d point sets," *IEEE Transactions on pattern analysis and machine intelligence*, no. 5, pp. 698–700, 1987.

[6] F. Nyssen and J.-C. Golinval, "Identification of mistuning and model updating of an academic blisk based on geometry and vibration measurements," *Mechanical Systems and Signal Processing*, vol. 68, pp. 252–264, 2016.